Prolylcarboxypeptidase regulates food intake by inactivating α-MSH in rodents

Nicholas Wallingford,[1] Bertrand Perroud,[2] Qian Gao,[1] Anna Coppola,[1] Erika Gyengesi,[1] Zhong-Wu Liu,[1] Xiao-Bing Gao,[1] Adam Diament,[3] Kari A. Haus,[3] Zia Shariat-Madar,[4] Fakhri Mahdi,[4] Sharon L. Wardlaw,[5] Alvin H. Schmaier,[6] Craig H. Warden,[3] and Sabrina Diano[1,7]

[1]Department of Obstetrics, Gynecology, and Reproductive Sciences, Yale University School of Medicine, New Haven, Connecticut, USA. [2]Genome Center and [3]Rowe Program in Genetics, Department of Pediatrics and Department of Neurobiology, Physiology, and Behavior, University of California Davis, Davis, California, USA. [4]Department of Pharmacology, University of Mississippi, Oxford, Mississippi, USA. [5]Department of Medicine, Columbia University College of Physicians and Surgeons, New York, New York, USA. [6]Department of Medicine, Case Western Reserve University, Cleveland, Ohio, USA. [7]Department of Neurobiology, Yale University School of Medicine, New Haven, Connecticut, USA.

The anorexigenic neuromodulator α-melanocyte–stimulating hormone (α-MSH; referred to here as α-$MSH_{1–13}$) undergoes extensive posttranslational processing, and its in vivo activity is short lived due to rapid inactivation. The enzymatic control of α-$MSH_{1–13}$ maturation and inactivation is incompletely understood. Here we have provided insight into α-$MSH_{1–13}$ inactivation through the generation and analysis of a subcongenic mouse strain with reduced body fat compared with controls. Using positional cloning, we identified a maximum of 6 coding genes, including that encoding prolylcarboxypeptidase (PRCP), in the donor region. Real-time PCR revealed a marked genotype effect on *Prcp* mRNA expression in brain tissue. Biochemical studies using recombinant PRCP demonstrated that PRCP removes the C-terminal amino acid of α-$MSH_{1–13}$, producing α-$MSH_{1–12}$, which is not neuroactive. We found that *Prcp* was expressed in the hypothalamus in neuronal populations that send efferents to areas where α-$MSH_{1–13}$ is released from axon terminals. The inhibition of PRCP activity by small molecule protease inhibitors administered peripherally or centrally decreased food intake in both wild-type and obese mice. Furthermore, *Prcp*-null mice had elevated levels of α-$MSH_{1–13}$ in the hypothalamus and were leaner and shorter than the wild-type controls on a regular chow diet; they were also resistant to high-fat diet–induced obesity. Our results suggest that PRCP is an important component of melanocortin signaling and weight maintenance via control of active α-$MSH_{1–13}$ levels.

Introduction

Analysis of congenic mouse strains provides a general method to identify genes for complex traits using positional genetics tools. Congenic mouse strain analyses have successfully identified several positional candidate obesity genes (1–3). The identification of novel aspects of known metabolic pathways is a particularly valuable outcome of positional genetics approaches.

The prohormone proopiomelanocortin (POMC) plays a critical role in the regulation of energy metabolism. POMC is processed by proteases to produce several peptide hormones, including α-melanocyte–stimulating hormone (α-MSH, here referred to α-$MSH_{1–13}$). α-$MSH_{1–13}$ is a critical anorexigenic neuromodulator in the hypothalamus. It inhibits food intake by binding target neurons expressing melanocortin receptors 3 and 4 (MC3R and MC4R; reviewed in ref. 4).

α-$MSH_{1–13}$ is generated through extensive posttranslational processing that involves several enzymes such as prohormone convertases 1 and 2 (PC1 and PC2), carboxypeptidase E (CPE), and peptidyl α-amidating monooxygenase (PAM; reviewed in ref. 5). Once produced, α-$MSH_{1–13}$ undergoes a maturation process: desacetylated α-$MSH_{1–13}$ (Des-α-$MSH_{1–13}$) is converted to *N*-acetylated α-$MSH_{1–13}$ (Act-α-$MSH_{1–13}$) by an *N*-acetyltransferase that has not yet been identified (5, 6). The acetylation of α-$MSH_{1–13}$ may serve as a protective measure that stabilizes the peptide against degradation to prolong its action on target cells. Nevertheless, the ability of α-$MSH_{1–13}$ to reduce food intake is short lived and only effective when administered i.c.v. To date, the enzyme responsible for the rapid inactivation of α-$MSH_{1–13}$ is unknown.

Recently, we identified a B6.C-*D7Mit353* subcongenic mouse line with less body fat than its B6By background control line (7). Phenotypic differences (such as obesity) between these background and congenic strains are due to polymorphisms in genes located in the congenic donor region located on chromosome 7. We identified prolylcarboxypeptidase (*Prcp*) as the candidate gene responsible for our congenic phenotype. The enzyme, PRCP, is a serine protease that cleaves small, biologically active peptides at carboxyl termini linked to a penultimate proline, Pro-X. Thus, because of its C-terminal amino acid sequence Pro-Val, α-$MSH_{1–13}$ is a putative substrate of PRCP. This study was undertaken to determine the role of PRCP in food intake and energy balance regulation.

PRCP initiates the degradation and inactivation of extracellular α-$MSH_{1–13}$. We found that *Prcp* was expressed in neuronal populations that send efferents to areas where α-$MSH_{1–13}$ is released from axon terminals. We show that α-$MSH_{1–13}$ is a substrate of PRCP and that PRCP-degraded α-$MSH_{1–13}$ (α-$MSH_{1–12}$) is not neuroactive. Inhibition of PRCP activity by small molecule protease inhibitors administered peripherally or centrally decreased food intake in wild-type as well as genetically obese animals. Furthermore, *Prcp*-null mice had elevated hypothalamic levels of α-$MSH_{1–13}$ and

Conflict of interest: The authors have declared that no conflict of interest exists.

Nonstandard abbreviations used: ACTH, adrenocorticotropic hormone; AI, adiposity index; BPP, t-butyl carbamate–prolyl prolinal; DMH, dorsomedial nucleus of the hypothalamus; Hcrt, hypocretin/orexin; HFD, high-fat diet; HK, high-molecular-weight kininogen; LH, lateral hypothalamus; MC3R, melanocortin 3 receptor; MCH, melanin-concentrating hormone; MTII, Ac-Nle[4]-c[Asp[5], D-Phe[7], Lys[10]] α-MSH-(4-10)-NH_2; PK, prekallikrein; POMC, proopiomelanocortin; PRCP, prolylcarboxypeptidase; PVN, paraventricular nucleus; ZPP, *N*-benzyloxycarbonyl-prolyl-prolinal.

Citation for this article: *J. Clin. Invest.* **119**:2291–2303 (2009). doi:10.1172/JCI37209.

Table 1
Phenotypic association of *Prcp*$^{gt/gt}$ and congenic mice

	Congenic B6.C-*D7Mit353*		Congenic B6.C-*D7Mit373*		*Prcp*$^{gt/gt}$	
Phenotype	**Fold change**	***P***	**Fold change**	***P***	**Fold change**	***P***
Body weight	1.00	0.449	0.97	0.106	0.90	0.008
Body length	1.00	0.450	0.98	0.410	0.95	0.003
Femoral WAT	0.76	0.009	0.76	0.035	0.45	4×10^{-6}
Gonadal WAT	0.78	0.018	0.79	0.039	0.38	3×10^{-7}
Mesenteric WAT	0.82	0.069	0.72	0.023	0.56	8×10^{-6}
Retroperitoneal WAT	0.88	0.227	0.70	0.016	0.61	0.0001
BMI	0.98	0.270	1.00	0.499	0.95	0.043
Total fat	0.80	0.030	0.76	0.027	0.53	4×10^{-6}
AI	0.80	0.023	0.78	0.023	0.59	2×10^{-6}

Congenic mice and *Prcp*$^{gt/gt}$ have significantly less femoral, gonadal, mesenteric, and retroperitoneal white adipose tissue, resulting in lower total fat values, as well as a lower AI, compared with background or control mice. Fold changes were calculated in comparison between *Prcp*$^{gt/gt}$ and wild-type mice or between congenic and background strains. *P* values were calculated with Student's *t* tests. Sample sizes were as follows: B6.C-*D7Mit353*, *n* = 49 congenic, *n* = 32 background; B6.C-*D7Mit373*, *n* = 25 congenic, *n* = 28 background; *Prcp*$^{gt/gt}$, *n* = 19 KO, *n* = 14 wild-type. Average animal age was 121 days, with a range of 116–126 days.

were leaner compared with wild-type controls when exposed to a regular chow or high-fat diet (HFD). Our results suggest that PRCP is an important component of melanocortin signaling because it controls the levels of active α-$MSH_{1–13}$.

Results

Identification of PRCP as a positional candidate gene for the B6.C-D7Mit353 congenic strain. Our congenic strain contains the *D7Mit353* BALB/c allele (congenic line name B6.C-*D7Mit353*) on chromosome 7. In this congenic strain, DNA from the donor BALB/c strain is surrounded by background C57BL/6ByJ (B6By) genomic DNA (7). The BALB/c maximal donor region is between *D7Mit301* and *D7Mit96*, because both of these markers have the B6By alleles in the congenic animals. This donor region spans approximately 8 Mb and includes about 70 genes that may have BALB/c alleles (7). The B6.C-*D7Mit353* strain is leaner than the background B6By strain, with about 25% less femoral and gonadal white adipose tissue and respective *t* test *P* values of 0.009 and 0.018 (Table 1 and Supplemental Table 1; supplemental material available online with this article; doi:10.1172/JCI37209DS1). This is reflected by an adiposity index (AI) of 80% of the B6By strain, with a *P* value of 0.023. Mesenteric and retroperitoneal white adipose tissues were also measured but did not yield statistically significant results, nor was there a significant difference in BMI.

We derived 3 new subcongenic mouse strains from the B6.C-*D7Mit353* strain. These new strains were selected to include BALB/c alleles of *D7Mit373* (proximal), *D7Mit321* (middle), and *D7Mit354* (distal). Effects of genotype on obesity were determined in F_2 littermates of congenic × background strain crosses. The results revealed significant genotype effects on obesity in the B6.C-*D7Mit373* strain, with an AI of 78% of the B6By strain (*t* test *P* = 0.023; see Table 1 and Supplemental Table 1), but there were no significant effects in the other two strains.

Mapping of the congenic donor region by sequencing and identification of BALB/c SNPs has revealed that the B6.C-*D7Mit373* congenic region includes 4 genes that encode proteins: *Pcf11*, *Rab30*, *Prcp*, and *A830059I20Rik* (NM_021427; EG58238). In addition to the BALB/c allele of the marker *D7Mit373,* these 4 genes have been confirmed by sequencing to be BALB/c alleles (see Supplemental Table 2 for SNPs; Supplemental Table 3 for accession numbers for BALB/c and B6By; and Supplemental Table 4 for sequencing primers), while *Odz4* has been confirmed as an allele of the background B6By strain and thus is just outside of the B6.C-*D7Mit373* donor region.

We focused our studies on *Prcp* (also listed as angiotensinase C or Pro-X carboxypeptidase-related), an endopeptidase located in the donor region of both B6.C-*D7Mit353* and B6.C-*D7Mit373* congenic strains, because it has previously been associated with metabolic syndrome in human males (8). It is also conceptually related to CPE, which is the underlying cause of the "fat" mutation in mice (9–11). No other functional obesity candidate genes are located in the B6.C-*D7Mit373* donor region.

Real-time PCR of PRCP in the brain. We hypothesized that if *Prcp* is the gene underlying the obesity phenotype in our congenic mice, it may have differential expression in background and congenic strains. We determined Prcp expression levels in whole-brain tissue mRNA extracts using real-time PCR. One SYBR green probe (targeting exon 5) and 3 TaqMan probes (targeting the exons 2, 3, and 6) were utilized to assay Prcp expression (Figure 1). We found 0.53 ± 0.11–fold (mean ± SD) lower expression of Prcp in brains of B6.C-*D7Mit353* homozygous congenic mice compared with mice of the background strain, 0.82 ± 0.04–fold lower expression in heterozygous congenic mice compared with background mice, and 0.64 ± 0.15–fold lower expression in homozygous B6.C-*D7Mit353* compared with heterozygous congenic mice. We observed statistically significant *P* values, from 6×10^{-3} to 5×10^{-6} (Supplemental Table 5). These results are consistent with an additive model in which the background allele causes increased Prcp expression.

Sequencing of Prcp in the background and congenic mice. To search for functional differences between background and congenic alleles of *Prcp*, we sequenced both the donor and background alleles of *Prcp*. No coding, 3′ UTR, or 5′ UTR variants were found. One promoter base change, a C→T transition in the donor strain, was found. This base change is located –718 bases upstream of the start codon (see Supplemental Table 4 for sequencing primers).

PRCP gene trap mice confirm the PRCP obesity phenotype. We next produced *Prcp* gene trap (*Prcp*$^{gt/gt}$) mice to confirm that a variation in PRCP expression causes obesity. Gene trap mice lacking expression of PRCP were created by insertion of the CD4-TM-βgeo reporter

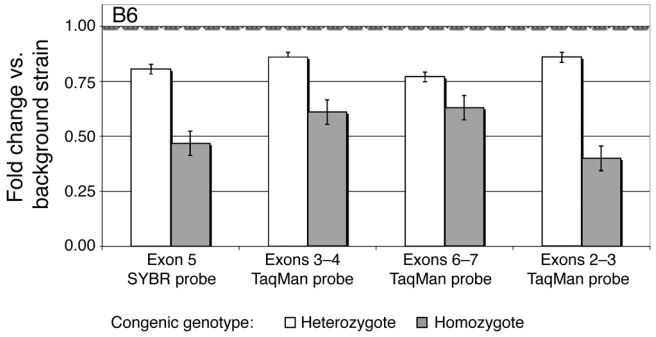

Figure 1
RT-PCR for quantitation of *Prcp* in brain. PRCP real-time PCR in brain of B6.C-*D7Mit353* congenic mice using probes targeting exons 5, 3–4, 6–7, and 2–3. The results for heterozygous and homozygous congenic mice are expressed as fold changes relative to the background strain (represented by a value of 1.00). Data represent the mean ± SEM. Ct means and SDs are available in Supplemental Table 5.

cassette into intron 4 of mouse *Prcp* (Figure 2A) (12). DNA from the heterozygous KST302 parent cell line showed significantly more *lacZ* expression on real-time PCR than that from KST302 ES cells heterozygous for the PRCP gene trap (Figure 2, A and B). In studies on mRNA from kidneys of $Prcp^{gt/gt}$ and wild-type mice, the insertion of the gene trap was localized to intron 4 (Figure 2, A, C, and D). These mice were backcrossed to C57BL/6J mice for 10 generations to produce knockout/congenic mice. Further details on the generation and genetic characterization of these animals can be found in Methods and Supplemental Table 6. Minimal expression of PRCP mRNA was detected in the hypothalamus and kidney of $Prcp^{gt/gt}$ mice (0.02 ± 0.003–fold change in expression in hypothalamus and 0.09 ± 0.009–fold change in the kidney) compared with wild-type controls (1.00 ± 0.02– and 1.06 ± 0.18–fold change in expression in hypothalamus and kidney, respectively; Figure 2, E and F).

A significant decrease in body, total, and individual fat pad weights was observed in $Prcp^{gt/gt}$ compared with wild-type control mice on a regular chow diet (Table 1 and Supplemental Table 1). In addition, $Prcp^{gt/gt}$ mice showed a significantly decreased body length, BMI, and AI (Table 1 and Supplemental Table 1). Analysis of their daily average food intake showed that $Prcp^{gt/gt}$ mice ate significantly less (3.08 ± 0.09 g/d) than age-matched wild-type controls (3.58 ± 0.9 g/d). Significant reductions in body weight, body length, BMI, AI, and food intake were also observed in female $Prcp^{gt/gt}$ mice compared with wild-type controls (data not shown).

When we exposed $Prcp^{gt/gt}$ mice to a HFD (45% fat), a significant difference in body weight was also observed between $Prcp^{gt/gt}$ and wild-type mice from the first week of the HFD regimen. $Prcp^{gt/gt}$ mice display a lower body weight compared with wild-type controls. This difference was evident for the entire period of exposure to the diet (18 weeks; Figure 3A). To examine whether the difference in body weight was due to a differential energy intake, food intake was measured weekly. $Prcp^{gt/gt}$ mice ate significantly less than wild-type controls (Figure 3B). Finally, when we analyzed body composition of the animals exposed to HFD for 18 weeks, we found a significantly ($P = 0.03$) lower percentage of fat mass in $Prcp^{gt/gt}$ mice (36.3% ± 0.6%) compared with wild-type controls (39.4% ± 0.9%). No difference ($P = 0.07$) in lean mass was observed between $Prcp^{gt/gt}$ mice (55.9% ± 0.5%) and wild-type animals (54.1% ± 0.7%). Thus, our results in $Prcp^{gt/gt}$ mice confirmed *Prcp* as a positional candidate in the B6.C-*D7Mit353* and B6.C-*D7Mit373* congenics and associate *Prcp* with the observed lean phenotype in our congenic mice. We have also demonstrated that decreased expression of *Prcp* causes decreased obesity in mice.

α-$MSH_{1–13}$ is a substrate of PRCP. Because of the penultimate proline in its amino acid sequence, α-$MSH_{1–13}$ is a putative substrate of PRCP. We performed an in vitro assay to determine whether α-$MSH_{1–13}$ is a substrate inhibitor of $rPRCP_{51}$-induced prekallikrein (PK) activation (Figure 3C) (13, 14). Recombinant $PRCP_{51}$ activates PK with a K_m and V_{max} of 9 nM and 0.2 min^{-1}, respectively (13). Incubation of PRCP with α-$MSH_{1–13}$ at 0.001 to 1 mM led to a gradual decrease in the activation of PK by $rPRCP_{51}$, with an IC_{50} of 100 μM. Likewise, Ang II, an established substrate of PRCP, inhibited PK activation with an IC_{50} of 150 μM, as was shown previously (13–15). In contrast, the putative product of PRCP hydrolysis of α-$MSH_{1–13}$, $MSH_{1–12}$, was much less effective in blocking $rPRCP_{51}$ activity, achieving approximately 20% inhibition at 1 mM (Figure 3C). These data show that α-$MSH_{1–13}$ with its C-terminal Pro-Val bond, but not $MSH_{1–12}$, which lacks the C-terminal Val, is a substrate of PRCP.

Effect of peripheral α-$MSH_{1–13}$ administration in $Prcp^{gt/gt}$ mice. Despite α-$MSH_{1–13}$'s well-described anorectic function and the recognition of MC4R as its critical mediator (10, 16), peripheral administration of α-$MSH_{1–13}$ has not been reported to reduce food intake. In contrast, a synthetic analog of melanocortins, Ac-Nle^4-c[Asp^5, D-Phe^7, Lys^{10}] α-MSH-(4-10)-NH_2 (MTII), is readily able to reduce food intake even after peripheral administration (16). The lack of effect on food intake of peripheral α-$MSH_{1–13}$ suggests that extracellular degradation of α-$MSH_{1–13}$ is an important element in determining its anorexigenic efficacy (6). Since PRCP is expressed in various peripheral tissues, it is likely that peripherally administered α-$MSH_{1–13}$ is degraded before it can reach its targets in the central nervous system. To further test whether α-$MSH_{1–13}$ is a substrate of PRCP, we assessed the effect of peripheral α-$MSH_{1–13}$ administration on food intake in wild-type and $Prcp^{gt/gt}$ mice and compared these values with those obtained by peripheral MTII administration.

Intraperitoneal injection of α-$MSH_{1–13}$ (200 nmol) into wild-type mice had no effect on feeding (1.11 ± 0.06 g saline versus 0.89 ± 0.13 g α-MSH; Figure 3D), while MTII (200 nmol) administration resulted in a significant decline in food intake (0.15 ± 0.04 g; Figure 3D) 4 hours after administration. However, i.p. injection of α-$MSH_{1–13}$ (200 nmol) into $Prcp^{gt/gt}$ mice had a significant effect on food intake reduction (1.21 ± 0.09 g saline versus 0.48 ± 0.06 g α-$MSH_{1–13}$ versus 0.17 ± 0.04 g MTII; Figure 3E). Because PRCP is expressed in various peripheral tissues as well as in the brain, we suggest that PRCP is responsible for inactivation of peripherally injected α-$MSH_{1–13}$ regarding food intake regulation.

α-$MSH_{1–12}$ is the product of PRCP action on α-$MSH_{1–13}$. We then exposed purified α-$MSH_{1–13}$ (MW, 1,665 Da) to $rPRCP_{51}$ for a period of 1 hour at 37°C to study the products of the reaction of PRCP with α-$MSH_{1–13}$ by liquid chromatography–mass spectrometry (LC-MS). A control sample was made by stopping the reaction immediately after adding the substrate α-$MSH_{1–13}$ (Figure 4A, top and middle panels). The reaction mixes were analyzed by LC-MS on a Fourier transform mass spectrometry instrument. A new peak appeared at a shorter retention time in the 1-hour–incubated samples (Figure 4B, top panel). MS spectrum analysis of a 1-hour-incubation sample showed the almost complete disappearance of α-$MSH_{1–13}$ (Figure 4B, middle panel) and the appearance of a new compound (Figure 4B, bottom panel) with a spectrum matching α-$MSH_{1–12}$ standard triply charged ion isotopic masses and α-$MSH_{1–12}$ theoretical size (MW, 1,566 Da). This compound was not present in the control samples (Figure 4A,

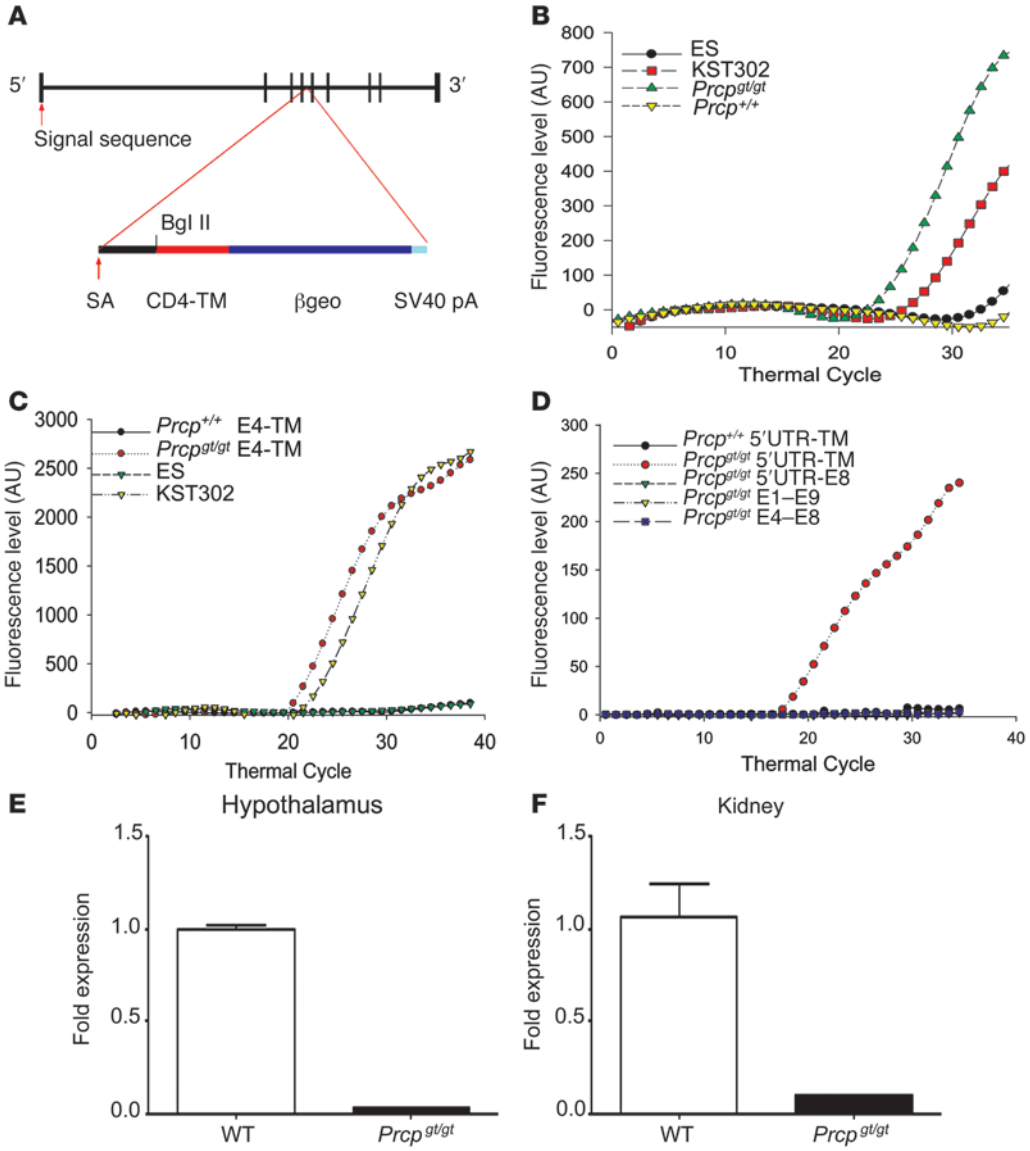

Figure 2

Generation and characterization of *Prcp*$^{gt/gt}$ mice. (**A**) The gene trap method of generating *Prcp*$^{gt/gt}$ mice involved a βgeo targeting vector randomly incorporating into intron 4. The CD4-TM-βgeo incorporated into genes with a signal sequence allowed for LacZ expression and interruption of PRCP expression. These interruptions were screened with X-gal staining. SV40 pA, SV40 polyadenylation signal. (**B**) Real-time PCR analysis was performed to screen for *LacZ* expression in *Prcp*$^{gt/gt}$ and *Prcp*$^{+/+}$ mice, in wild-type cells (ES), or in a *PRCP* gene–trapped PRCP cell line (KST302). Shown are representative real-time PCR results for 1 mouse and 1 cell DNA sample (n = 5 mice). (**C**) Real-time PCR from kidney of *Prcp*$^{gt/gt}$ or *Prcp*$^{+/+}$ mice or ES or KST302 cells around the insertional mutation site using sense primers to exon 4 of PRCP and antisense primers to the TM region of pGT1TM vector and a probe common to the contiguous sequence of exon 4 with the splicing acceptor (SA) region of pGT1TM vector. The figure shows representative results for the wild-type (n = 5) and *Prcp*$^{gt/gt}$ mice (n = 5) included in the experiment shown in **B**. (**D**) Real-time PCR from kidneys of *Prcp*$^{gt/gt}$ or *Prcp*$^{+/+}$ mice using a probe that spans the 3′ region of exon 4 and splice acceptor region of the vector of the cDNA using various combinations of sense and antisense primers of *Prcp*. The figure is a representative experiment on a single mRNA specimen (20 experiments performed in total). (**E** and **F**) Graphs showing the results of real-time PCR for *Prcp* in hypothalamic and kidney samples from *Prcp*$^{gt/gt}$ mice and wild-type controls. Data represent the mean ± SEM.

bottom panel). Thus, we have demonstrated that PRCP reaction with α-MSH$_{1–13}$ under steady-state kinetic conditions, liberated the terminal Valine of α-MSH$_{1–13}$ to generate α-MSH$_{1–12}$.

α-MSH levels are increased in the hypothalamus of Prcp$^{gt/gt}$ *mice.* To assess whether PRCP regulates α-MSH levels in vivo, we next measured the levels of α-MSH in the hypothalami of wild-type and *Prcp*$^{gt/gt}$ mice. A significant increase in α-MSH was observed in the hypothalamus of *Prcp*$^{gt/gt}$ mice (225.6 ± 35.14 fmol/mg protein) compared with wild-type controls (129.7 ± 17.10; Figure 4C). Additionally, a significant difference in α-MSH/adrenocorticotropic hormone (α-MSH/ACTH) ratio between *Prcp*$^{gt/gt}$ mice (1.92 ± 0.22) and wild-type controls (1.24 ± 0.16) was observed (Figure 4D). No significant difference in α-MSH plasma levels between wild-type and *Prcp*$^{gt/gt}$ mice was found (data not shown).

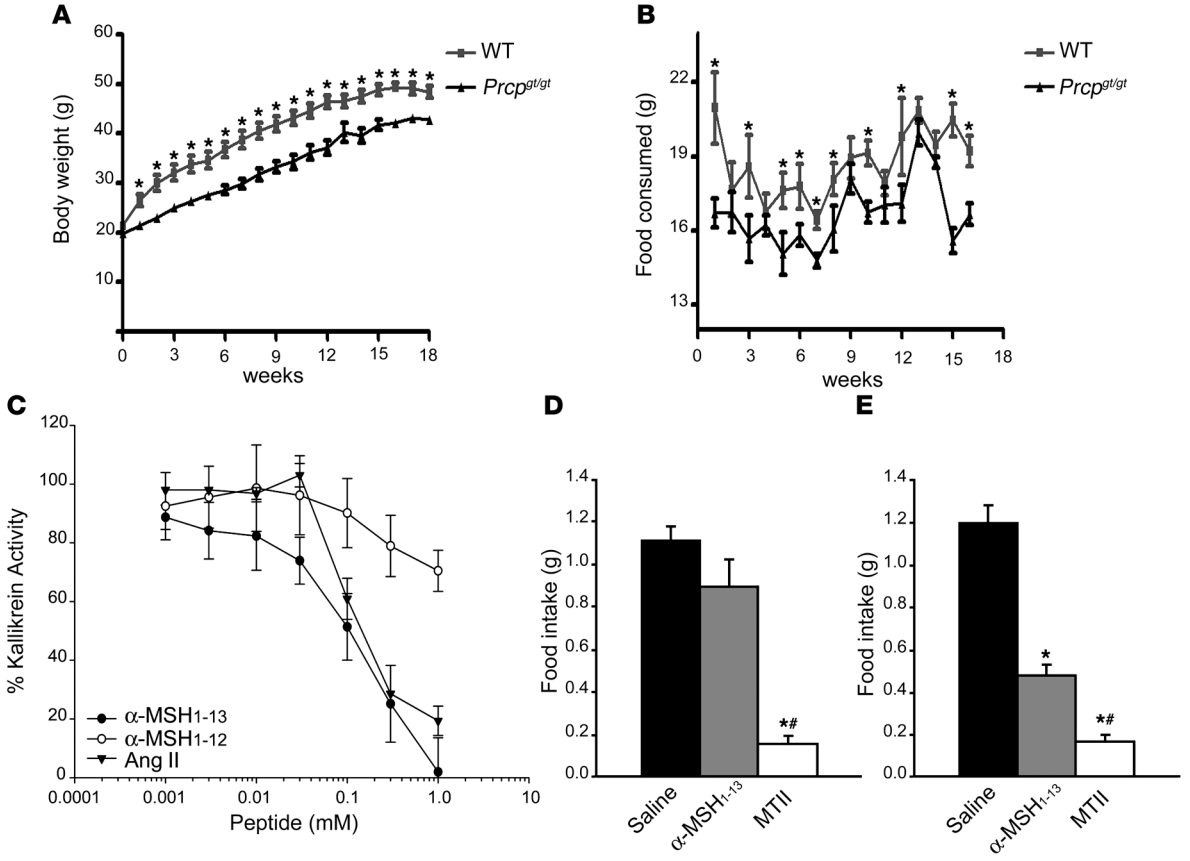

Figure 3

α-MSH is a substrate of PRCP. (**A** and **B**) Changes in body weight and food intake of *Prcp*$^{gt/gt}$ mice and wild-type controls exposed to HFD. Data represent the mean ± SEM. (**C**) Increasing concentrations of α-MSH$_{1–13}$, α-MSH$_{1–12}$, or Ang II (0.001–1 mM) were incubated with 8 nM of rPRCP$_{51}$ at 37°C in microtiter plate cuvette wells with preabsorbed HK and containing 20 nM PK. The liberation of paranitroanilide (pNA) from the S2302 by the formed plasma kallikrein in the presence of the peptide was measured at 405 nm. Results are expressed as residual formed plasma kallikrein activity. The data represent the mean ± SEM of 3 independent measurements. (**D** and **E**) Food intake in grams 4 hours after an i.p. injection of 200 nmol of α-MSH$_{1–13}$ or 200 nmol of MTII in wild-type (**D**) or *Prcp*$^{gt/gt}$ mice (**E**) compared with saline-injected control animals. Data represent the mean ± SEM. **P* < 0.001 compared with saline; #*P* < 0.001 compared with α-MSH.

PRCP expression in the hypothalamus. To clarify whether PRCP-expressing cells are present in the hypothalamus, we analyzed β-gal expression in hypothalamic slices in *Prcp*$^{gt/gt}$ mice. Expression of β-gal in the central nervous system was found to be abundant in various regions, including the cerebral cortex, brain stem, hippocampus, and hypothalamus. In the hypothalamus, β-gal–labeled cells were highly expressed in the lateral hypothalamus–perifornical (LH-perifornical) area and zona incerta (ZI) and dorsomedial nucleus (Figure 5A). Labeled cells were also found in the arcuate nucleus of the hypothalamus (Figure 5A). The expression of β-gal in *Prcp*$^{gt/gt}$ animals was virtually identical to the distribution pattern of PRCP mRNA in wild-type animals as revealed by in situ hybridization of PRCP mRNA (Figure 5B).

In one of the hypothalamic regions where PRCP is most abundantly expressed, the LH perifornical region, there are two known orexigenic peptidergic circuits that project to α-MSH$_{1–13}$–targeted sites: one producing melanin-concentrating hormone (MCH) and the other hypocretin/orexin (Hcrt; refs. 17–23). Double labeling studies revealed that populations of MCH and Hcrt neurons also expressed β-gal (Figure 5, C and D). β-Gal–labeled boutons were found in direct apposition to α-MSH–containing axon terminals in various parts of the hypothalamus, including the paraventricular nucleus (PVN) (Figure 5E). Finally, in the arcuate nucleus, the majority of POMC-immunolabeled cells lacked β-gal expression (Figure 5F), suggesting that if PRCP cleaves α-MSH$_{1–13}$, it should occur at α-MSH$_{1–13}$ release sites. These observations revealed that hypothalamic PRCP cells are in ideal anatomical position to affect α-MSH action.

Effect of α-MSH$_{1–13}$ and α-MSH$_{1–12}$ on food intake. To examine whether conversion of α-MSH$_{1–13}$ to α-MSH$_{1–12}$ by PRCP could affect food intake, we compared the effects of their i.c.v. administration on food intake. In overnight-fasted animals, 2.5 μg of α-MSH$_{1–13}$ induced a 40% reduction in food intake (5.21 ± 0.50 g) compared with saline-treated animals (8.71 ± 0.56 g; Figure 6A). On the other hand, 2.5 μg of α-MSH$_{1–12}$ did not significantly affect food intake (8.89 ± 0.90 g) compared with saline controls (Figure 6A).

Electrophysiologic effect of α-MSH$_{1–13}$ and α-MSH$_{1–12}$. The lack of suppression of food intake by α-MSH$_{1–12}$ suggests that the hydrolysis product of α-MSH$_{1–13}$ by PRCP is less active in regulating neuronal functions via melanocortin receptors. To test this hypothesis, we analyzed electrophysiological responses of MC4R-expressing neurons to α-MSH$_{1–13}$ and α-MSH$_{1–12}$ using patch clamp in vitro slice recordings from transgenic animals expressing GFP driven by the mouse MC4R

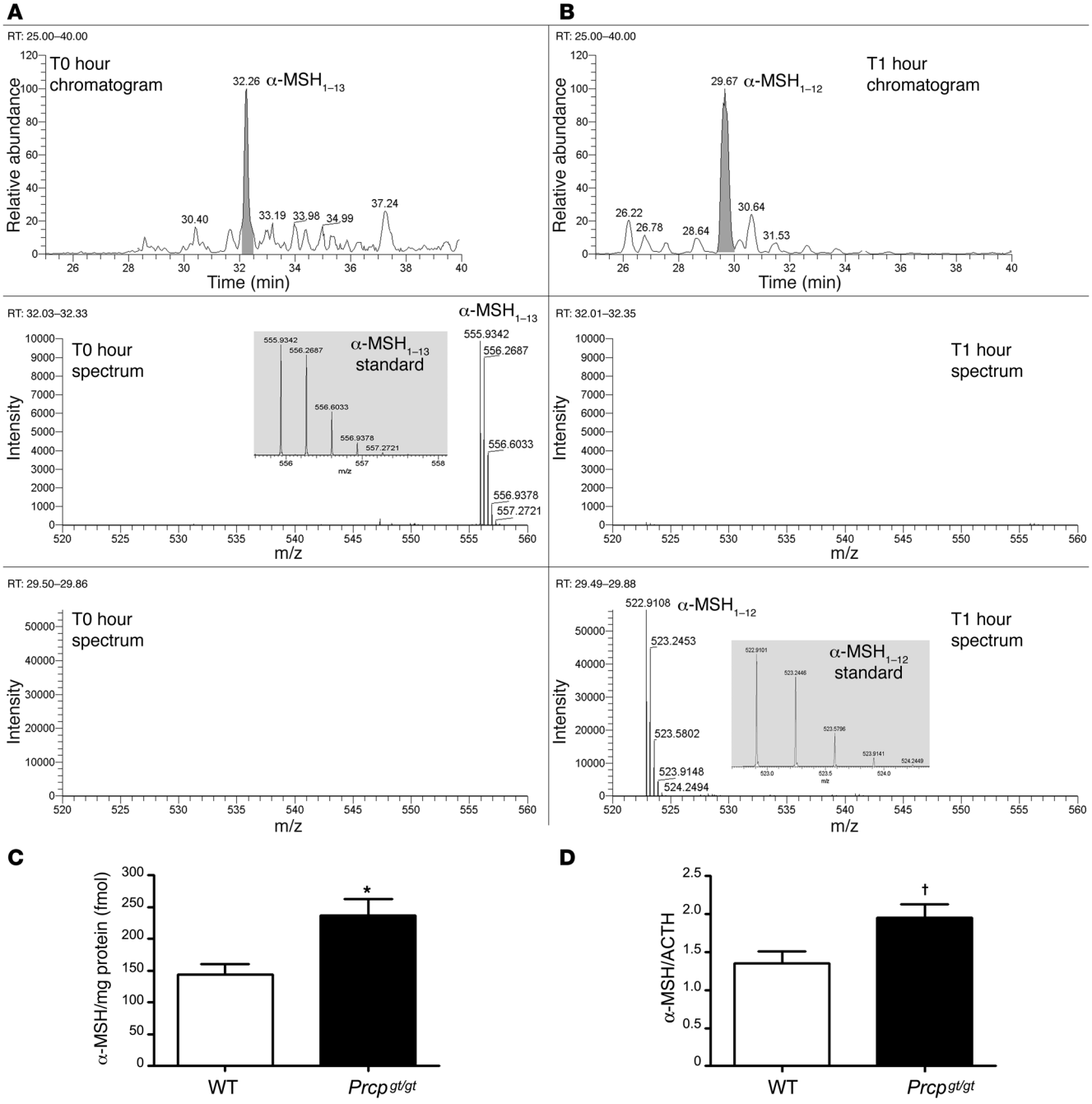

Figure 4

α-MSH levels in *Prcp*$^{gt/gt}$ mice. (**A** and **B**) Mass spectrometry analysis of products of the in vitro PRCP reaction with α-MSH$_{1–13}$. (**A**) Control (T0) analysis. (**B**) Liquid chromatography–mass spectrometry (LC-MS) analysis for the 1-hour incubation reaction (T1). The HPLC chromatogram base peaks are shown in the top panels for the retention time (RT) ranging from 25 to 40 minutes. A major peak eluting at 32 minutes (**A**, top panel, gray) has an MS spectrum perfectly matching the triply charged ion isotopic masses (middle panel) and α-MSH$_{1–13}$ theoretical size (MW, 1,665 Da). A new peak eluting at 30 minutes (**B**, top panel, gray) appears in the 1-hour reaction. Its MS spectrum matches the triply charged ion isotopic masses of α-MSH$_{1–12}$ standard (**B**, bottom panel) and its theoretical size (MW, 1,566 daltons). α-MSH$_{1–12}$ was not detected in the control samples (**A**, bottom panel). Standard spectra are shown overlaid in gray inserts. (**C**) α-MSH levels (expressed as fmol α-MSH/mg protein) in the hypothalamus of *Prcp*$^{gt/gt}$ mice ($n = 29$) compared with wild-type controls ($n = 14$). Data represent the mean ± SEM. *$P = 0.046$. (**D**) α-MSH/ACTH ratio in the hypothalamus of *Prcp*$^{gt/gt}$ mice compared with wild-type controls. Data represent the mean ± SEM. †$P = 0.047$.

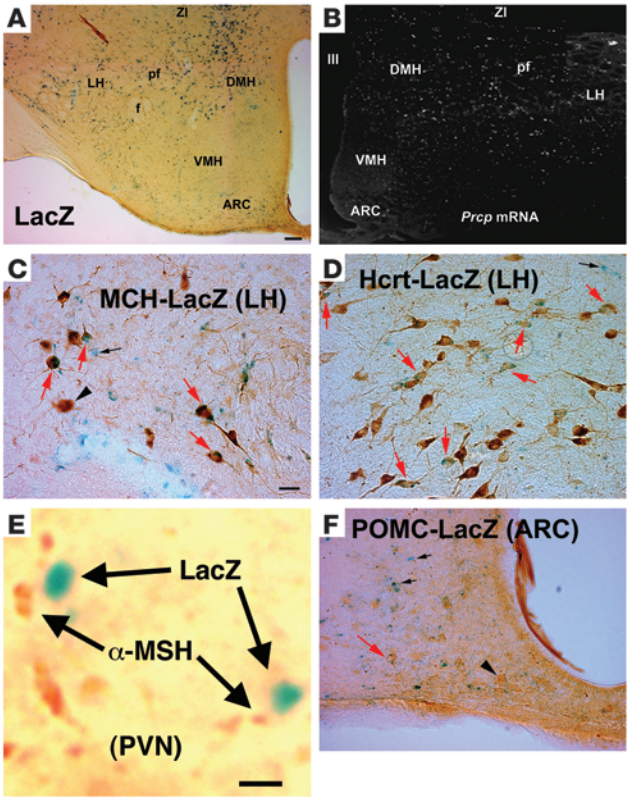

Figure 5
Hypothalamic localization of PRCP. (**A**) Dark blue β-gal labeling representing LacZ expression in the place of PRCP in cells of the hypothalamus. Most labeled cells are in the vicinity of the DMH, perifornical region (pf), LH, and zona incerta (ZI). A few labeled cells are also visible in the arcuate nucleus (ARC) of the mediobasal hypothalamus. f, fornix; III, third ventricle. (**B**) Corresponding to the LacZ expression shown in **A**, in situ hybridization for PRCP mRNA in wild-type animals resulted in labeled cells (dark-field micrograph; white dots represent digoxigenin labeling of antisense mRNA probe) in the DMH, pf, LH, and ZI, with a few labeled cells also present in the ARC. (**C**–**F**) Double labeling for β-gal (LacZ) and MCH or Hcrt revealed extensive coexpression of PRCP and MCH (**C**) and PRCP and Hcrt in the LH perifornical region (**D**). A few cells expressing POMC were also found to express LacZ (representing PRCP) in the arcuate nucleus (**F**). (**E**) LacZ-positive boutons in close proximity to α-MSH–immunopositive terminals in the hypothalamic PVN. Red arrows indicate double-labeled cells; black arrows point to single-labeled LacZ-expressing cells; and black arrowheads indicate single-labeled POMC, MCH, or Hcrt neurons. Scale bar in **A** (also applies to **B**): 100 μm. Scale bar in **C** (also applies to **D** and **F**): 10 μm. Scale bar in **E**: 2 μm.

promoter (24). Bath application of α-$MSH_{1–13}$ induced an increase in the frequency of action potential (221.7% ± 52.3%) that was restored to control levels after washing (147.8% ± 36.1%; Figure 6B). However, bath application of α-$MSH_{1–12}$ did not show any significant effect on MC4R (101.1% ± 21.1%; Figure 6C). This electrophysiological analysis confirmed that the hydrolysis product of α-$MSH_{1–13}$ by PRCP is ineffective in triggering adequate neuronal response.

Effect of PRCP inhibitors on food intake. If PRCP-regulated hydrolysis of α-$MSH_{1–13}$ has a physiological role in the regulation of food intake, then inhibition of PRCP enzymatic activity should interfere with feeding behavior. To test this, we analyzed the effect of two inhibitors on food intake: t-butyl carbamate–prolyl prolinal (BPP), a specific inhibitor of PRCP (gift of S. Wilk, unpublished observations), and *N*-benzyloxycarbonyl-prolyl-prolinal (ZPP), a previously characterized inhibitor of prolyl endopeptidase (PREP) and PRCP (14, 25).

Intracerebroventricular administration of BPP (0.9 μg) to rats suppressed overnight food intake (36.7% versus 94.91% of controls 24 hours after administration; Figure 6D). After 48 hours, when recovery of PRCP to control levels was achieved, detectable rebound feeding was not observed (89.24% versus 97.67% of controls; Figure 6D). We then administered BPP systemically (400 μg) to obese, leptin-deficient (*Lepob/ob*) mice and found that BPP also suppressed food intake in this animal model of hyperphagia (Figure 6E).

A dose-response curve of the effect of ZPP on food intake showed that in mice induced to feed by overnight food deprivation, ZPP produced potent inhibition of feeding within 1 hour of administration (Figure 6F). At the highest dose (100 mg/kg BW), food intake was inhibited for up to 8 hours after administration. A dose-response relationship between ZPP dose and feeding inhibition showed an ID_{50} at the 1-hour time point of 42.57 mg/kg BW. We also administered ZPP in *Lepob/ob* animals (100 mg/kg BW, i.p.) and found suppression of food intake in these hyperphagic animals (Figure 6G). These observations suggest that targeting PRCP activity with central or peripheral administration of protease inhibitors can reduce food intake.

ZPP-reduced feeding is mediated by melanocortin receptors. To further test the hypothesis that the inhibition of PRCP causes food reduction through the melanocortin receptors, we coadministered ZPP with the specific melanocortin antagonist and agouti mimetic SHU9119 (16). Inhibition of food intake in overnight-fasted mice by i.p. administration of 100 mg/kg of ZPP was blocked by coadministration of i.c.v. injected SHU9119 (Figure 6H). This result indicates that the effect of ZPP on feeding is caused by agonist binding of the product of PRCP reaction to MC4R and/or MC3R.

Discussion

The present study provides several independent types of evidence that PRCP is a candidate obesity gene involved in melanocortin signaling. We have shown that the small donor region in the B6.C-*D7Mit373* congenic strain contains 4 protein-coding genes and exhibits a lean phenotype. PRCP is the only gene from the congenic donor region with a statistically significant differential expression between BALB/c and B6By strains. Microarray data from brain, liver, gonadal white adipose tissue, and gastrocnemius muscle mRNA from the founding B6.C-*D7Mit353* strain also failed to reveal differential expression of any of the genes in the B6.C-*D7Mit373* subcongenic strain (our unpublished observations). The gene-trapped PRCP mice on a regular chow diet were leaner, as predicted by our congenic expression studies, and shorter than the wild-type controls, an indication of an increased melanocortin signaling in these animals. On a HFD, $Prcp^{gt/gt}$ mice also showed a significant reduction in body weight and a reduction in food intake. We have shown that α-$MSH_{1–13}$ is a substrate of PRCP and and expression of the latter in the hypothalamus is closely associated with areas of α-$MSH_{1–13}$ action in the hypothalamus. We have demonstrated that the product of α-$MSH_{1–13}$ degradation by PRCP in vitro is α-$MSH_{1–12}$, which is ineffective in reducing food intake and in regulating neuronal functions via

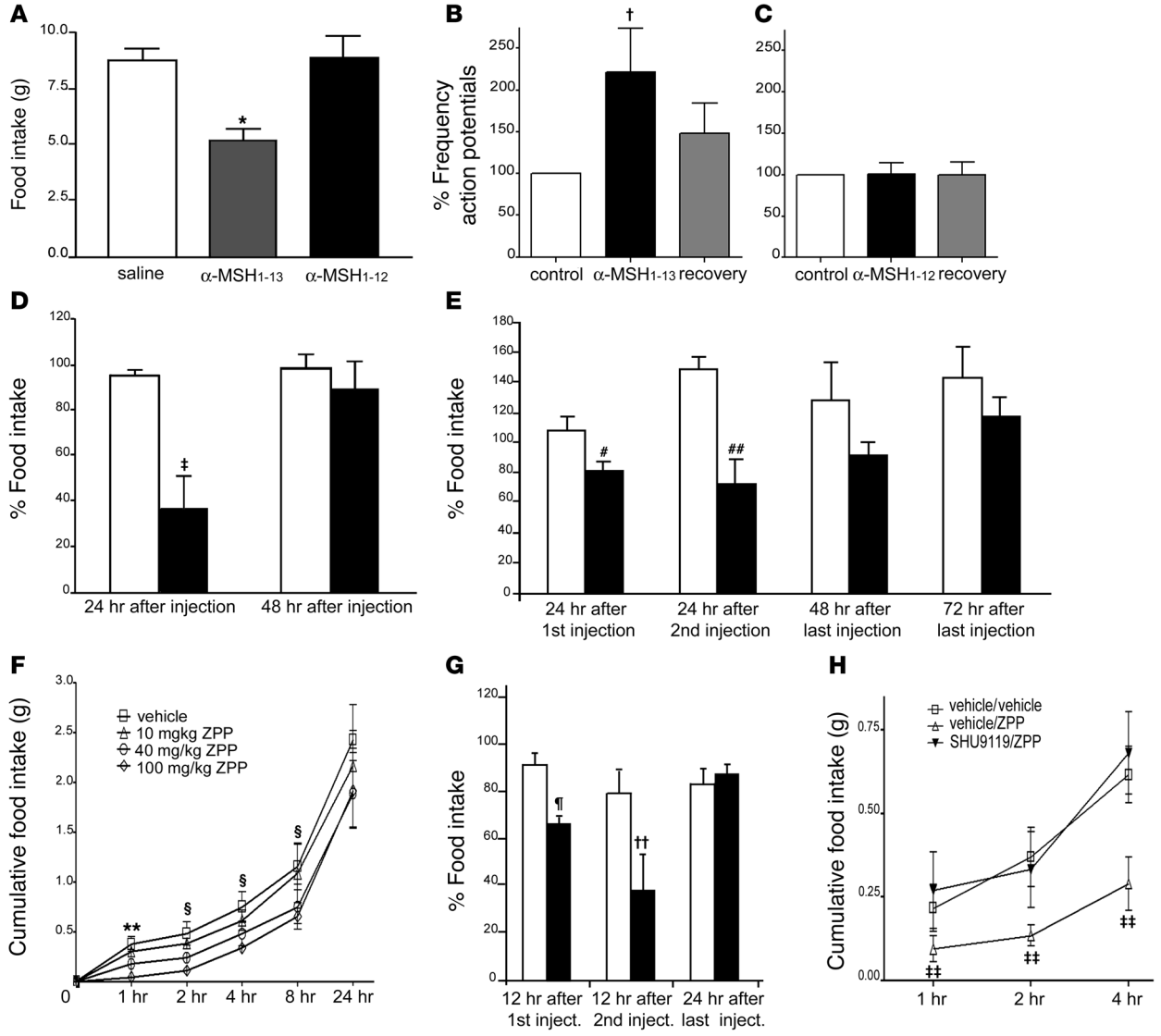

Figure 6

Effect of α-MSH$_{1-13}$ and α-MSH$_{1-12}$ on food intake. (**A**) Graph showing the effect of i.c.v. injection of 2.5 μg of α-MSH$_{1-13}$ and α-MSH$_{1-12}$ on food intake compared with saline control (n = 6 in both groups). Means (± SEM) were compared using 1-way ANOVA followed by the Student-Newman-Keuls method. $^{*}P$ = 0.006. (**B** and **C**) Electrophysiology results of α-MSH$_{1-13}$ (**B**) and α-MSH$_{1-12}$ (**C**) on GFP-MC4R neurons of the PVN of the hypothalamus (n = 9). Data represent the mean ± SEM. $^{\dagger}P$ = 0.024. (**D**) Effect of i.c.v. administration of vehicle and 0.9 mg BPP on food intake of fasted rats (n = 6 for each group). Data represent the mean ± SEM. Statistical analysis was performed by unpaired t test. $^{\ddagger}P$ = 0.016. (**E**) Percentage of food intake in *Lepob*/*ob* mice injected i.p. with vehicle (white bars; n = 5) and with 400 μg of BPP (black bars; n = 5). Data represent the mean ± SEM. Statistical analysis was performed by unpaired t test. $^{\#}P$ = 0.022, $^{\#\#}P$ = 0.039. (**F**) Inhibitory effect on food intake of i.p. administration of ZPP. ZPP produced a specific dose-responsive inhibition of food intake in overnight-fasted mice. Significance value indicated for individual time points represents 100 mg/kg BW versus vehicle. Data represent the mean ± SEM. $^{**}P$ = 0.0025, $^{\S}P < 0.05$. (**G**) Percentage of food intake in *Lepob*/*ob* mice injected i.p. with vehicle (white bars; n = 5) and with 100 mg/kg BW of ZPP (black bars; n = 5). The data represent the mean ± SEM. Statistical analysis was performed by unpaired t test. $^{\P}P$ = 0.006, $^{\dagger\dagger}P$ = 0.047. (**H**) Intracerebroventricularly injected SHU9119 (6 nmol) specifically blocks ZPP inhibition of food intake. Significance value indicated for individual time point represents vehicle/ZPP versus SHU9119/ZPP. Data represent the mean ± SEM. $^{\ddagger\ddagger}P$ = 0.0025 for treatment and P = 0.0002 for time points.

melanocortin receptors. Furthermore, using an antiserum that specifically recognizes the amidated form of α-MSH and does not cross-react with its free acid form (26, 27), we have shown that *Prcp*$^{gt/gt}$ mice have increased hypothalamic levels of α-MSH when compared with wild-type controls. However, no difference in plasma α-MSH levels were observed in *Prcp*$^{gt/gt}$ mice compared with wild-type controls. Thus, if peripheral PRCP does not affect circulating α-MSH levels, our results showing the lack of an effect on food intake after peripheral α-MSH administration in wild-type mice suggest that the major contributor to α-MSH degradation is centrally expressed PRCP. Finally, we have shown that inhibitors of PRCP influence food intake via melanocortin receptors. While inhibitor studies can be confounded by side effects from other genes, the results are consistent with a role of

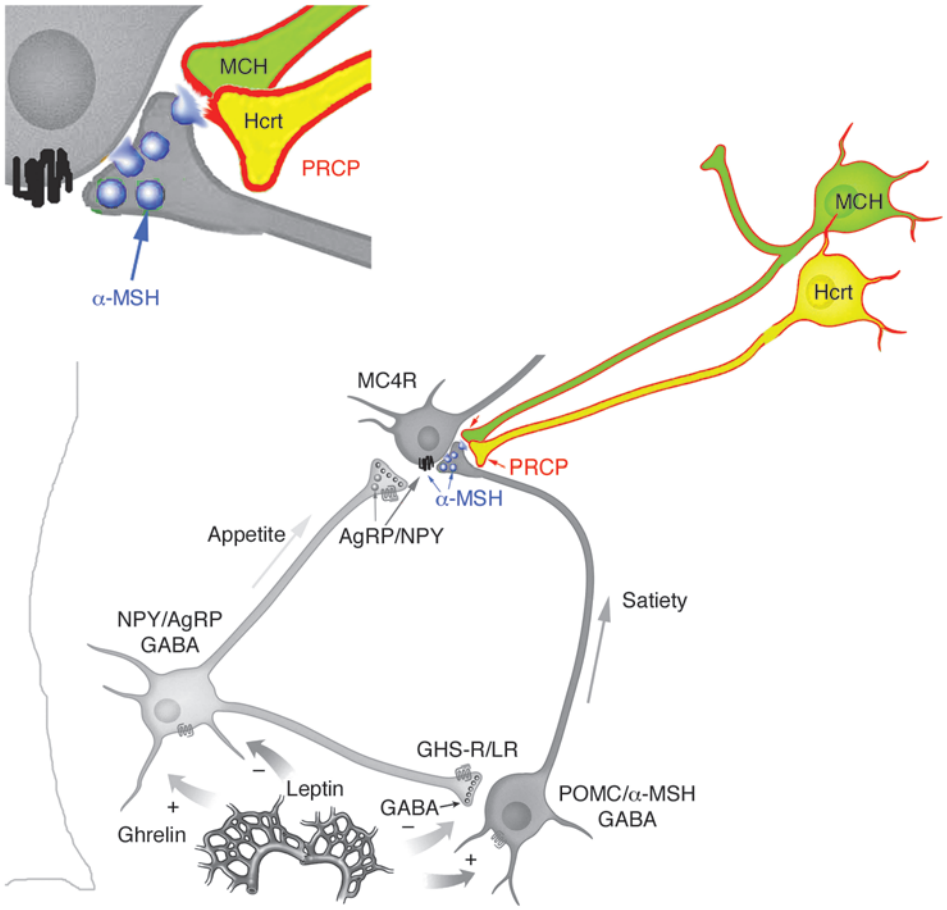

Figure 7
Schematic illustration showing that hypothalamic PRCP is in an anatomical position to determine the efficacy of released α-$MSH_{1–13}$, thereby controlling the output of the melanocortin system. We found that PRCP is mainly expressed in the lateral hypothalamic Hcrt and MCH neurons. These neurons project to various areas of the hypothalamus, such as the PVN, where α-$MSH_{1–13}$ terminals strongly innervate MC4R-expressing neurons. It is our hypothesis that PRCP, once released from the Hcrt and/or MCH terminals, will degrade α-MSH, thus increasing the antagonist effect of agouti-related protein (AgRP) and enhancing the orexigenic tone of the system. In support of this, congenic mice and *PRCP*$^{gt/gt}$ mice are leaner than the wild-type controls. GHS-R/LR, growth hormone secretagogue receptor/leptin receptor; NPY, neuropeptide Y.

PRCP in food intake. Taken together, these results indicate that expression of PRCP promotes obesity.

The functions of PRCP in regulating peptide actions in vivo have not been explored in detail. As a carboxypeptidase, PRCP catalyzes only the hydrolysis of the C-terminal peptide bond, releasing one amino acid. Although the cleavage of one amino acid from the C terminus of a peptide or protein might appear to be of limited importance, it often results in profoundly altered physiological activity of such molecules (28). Specifically, PRCP cleaves peptides only if the penultimate residue is proline. Our behavioral and electrophysiological results confirm that α-$MSH_{1–12}$ looses the effect of the parent peptide on food intake and on MC4R-containing neurons. In addition, it has been previously shown that PRCP retains substantial enzymatic activity at neutral pH with naturally occurring substrates, such as Ang II and PK, and is active extracellularly (13, 15, 29). Confirming these published studies, our in vitro results showed that at physiological pH, α-$MSH_{1–13}$ is a substrate of PRCP and that the degradation product of the reaction is α-$MSH_{1–12}$.

Our anatomical data suggest that hypothalamic PRCP is in an ideal position to determine the efficacy of released α-$MSH_{1–13}$, thereby controlling the output of the melanocortin system. We found that PRCP is mainly expressed in the dorsomedial nucleus of the hypothalamus (DMH) and in the lateral hypothalamic Hcrt and MCH neurons. These neurons project to various areas of the hypothalamus, such as the PVN, where α-$MSH_{1–13}$ terminals strongly innervate MC4R-expressing neurons.

While a relatively small number of MC4R-expressing neurons has been found in the LH, including the perifornical area (25), melanocortin axons have been shown to be widely distributed in the PVN and LH (30). Thus, it is plausible that α-$MSH_{1–13}$ may act presynaptically on MC4R-containing axon terminals arising from other sites of the central nervous system that project to the LH. Finally, high expression of MC4R-containing neurons has been shown in the hypothalamic DMH (25), where abundant expression of PRCP was detected and where arcuate α-$MSH_{1–13}$–containing fibers project (31). Thus, it is our hypothesis that PRCP acts in different hypothalamic sites to modulate melanocortin efficacy. Once released from the Hcrt and/or MCH terminals, PRCP will degrade α-$MSH_{1–13}$ extracellularly (Figure 7) and will also degrade α-$MSH_{1–13}$ intracellularly in the DMH, thus increasing the antagonist effect of agouti-related protein (AgRP) and enhancing the orexigenic tone of the system.

In summary, our data suggest that PRCP is a member of the validated melanocortin metabolic pathway. Future studies examining the regulation of PRCP in the hypothalamus will shed light on this new candidate target for the cure of obesity and related disorders.

Methods

Materials. α-$MSH_{1–13}$ (Ac-STSMEHFRWGKPV-NH_2) was purchased from Bachem (H1075), and Ang II was purchased from Phoenix Pharmaceuticals Inc. α-$MSH_{1–12}$ (Ac-STSMEHFRWGKP-COOH) was synthesized in its purified form by the W.M. Keck Foundation Biotechnology Resource Laboratory at Yale University. HD-Pro-Phe-Arg-paranitroanilide (S2302) was from DiaPharma. Human high-molecular-weight kininogen (HK)

(18 U/mg) and PK (21 U/mg) were obtained from Enzyme Research Laboratories. pMT/BiP/V5-His C was obtained from Invitrogen. ZPP was purchased from BIOMOL. BPP was a gift from Sherwin Wilk, Mount Sinai School of Medicine, New York, New York, USA.

Animal husbandry. All animal studies were approved by Yale University, University of California at Davis, Case Western Reverse University, and University of Mississippi Institutional Review Boards. Congenic and knockout mice were housed and cared for as reported previously (7). Briefly, once a subcongenic line was made, 2 heterozygous mice with the subcongenic region were mated, so that their progeny could serve as internal controls with random creation of each of the 3 possible genotypes. Thus, environmental variance was controlled for by using sibling mice as control mice. Mice were fed a low-fat diet, weaned at 3 weeks, and housed 5 per cage. Animals were euthanized at an average age of 121 days, with a range of 116–126 days. BMI was calculated as live fasted body weight/AN length in cm (AN is the length from tip of the nose to the anus). AI was calculated as summed weights of 4 fat pads (femoral [both], retroperitoneal [both], omental [one], and gonadal [one]) divided by live fasted body weight.

Total RNA extraction. At the time of mouse dissection, liver, spleen, brain, gastrocnemius muscle, kidneys, and 4 fat pads (femoral, epididymal, retroperitoneal, and mesenteric) were removed and flash frozen in liquid nitrogen. These samples were subsequently stored at –80°C before RNA extraction. Approximately 100 mg of sample tissue was used for RNA extraction using TRIzol (Life Technologies) according to the manufacturer's protocol.

Sequencing. Sequencing was done on cDNA for all but the 5′ UTR and 3′ UTR regions of the genes. For sequencing of the 5′ UTR and 3′ UTR, genomic DNA was used and primers were designed based on sequences from the mouse Celera database R13, which is currently incorporated into NCBI. Primers were used to amplify DNA and later to sequence the PCR fragment after a gel extraction using QIAquick Gel Extraction Kit (QIAGEN). These primers are listed in Supplemental Table 4. Primers were designed using the program EuGene version 2.2 (Daniben Inc.).

Reverse transcription. Single-stranded cDNA was synthesized using 1 μg of total RNA and a TaqMan reverse transcription kit (Applied Biosystems) according to the manufacturer's protocol.

Real-time PCR to quantitate Prcp mRNA in brain. RNA was isolated from male littermate mice derived from a cross of F_1 B6By and B6.C-*D7Mit353* mice. Whole brains were removed from mice after an overnight fast, and real-time PCR assays were performed in an Applied Biosystems 7900 Real-Time PCR System. Genotypes included the homozygous B6ByJ background strain ($n = 8$), the heterozygous strain ($n = 9$), and the homozygous BALB/cByJ congenic strain ($n = 7$). The TaqMan assays targeted a total of 6 separate exons of PRCP: TaqMan assay 814504 targets exons 3–4, TaqMan assay 814505 targets exons 6–7, and TaqMan assay 1324043 targets exons 2–3. In addition, a separate assay was performed using custom primers that were detected with SYBR green. Five separate control genes were used: 1 with SYBR green (36B4) and 4 with TaqMan. Genotype effects (deltas) were determined for all primers (Prcp and control genes). Values for the control genes were averaged. The overall fold of expression increase was calculated according to the manufacturer's instructions (Applied Biosystems).

Preparation of Prcp-knockout mice. ES cells (KST302) heterozygous for the *Prcp* gene trap were provided by William Skarnes (University of California at Berkeley, Berkeley, California, USA) through BayGenomics (NHLBI — Bay Area Functional Genomics Consortium; http://www.mmrrc.org/catalog/StrainCatalogSearchForm.jsp?pageSize=25&jboEvent=Search&SourceCollection=BayGenomics; ref. 12). The targeting vector (pGT1TM) containing a splice acceptor (SA) site, rat CD4 transmembrane domain, and a lacZ reporter sequentially was used to trap the *Prcp* gene in ES cells (12). The KST302 cells were microinjected into C57BL/6J blastocysts at the University of Michigan Transgenic Animal Model Core and surgically implanted in pseudopregnant female recipients on a 129/Sv background. Germline transmission was indicated by the presence of agouti coat color. Since the cloning vector contained a *lacZ* reporter gene, mice that contained a gene trap in PRCP were screened by real-time PCR using primers for LacZ (β-gal). At the time of the present experiments, $Prcp^{gt/gt}$ mice had been backcrossed 10 generations into a C57BL/6J background before homozygous mice were produced by breeding.

Characterization of $Prcp^{gt/gt}$ mice. Real-time quantitative PCR (TaqMan) analysis was carried out according to the manufacturer's instructions, with minor modifications. Briefly, measurements were performed using the iCycler iQ Real-Time PCR Detection System (Bio-Rad). Primers (Invitrogen) and probes (Integrated DNA Technologies) were designed. Probes were labeled with 6-carboxyfluorescein (FAM) and downstream 3′ Black Hole Quencher dye (BHQ-1; Integrated DNA Technologies) (Supplemental Table 6). Specific primers were used for the RT-PCR assay examining the insertional mutation site in kidney PRCP RNA. Melting profiles showed the generation of specific products with melting temperatures of 57.3°C. The PCR mixture (50 μl) consisted of 0.2 μM of each primer, 0.02 μM probe, 1 mg RNA, and TaqMan Universal Master Mix (2×) or Platinum Taq. The following reaction conditions were used: 95°C for 5 minutes, followed by 35 cycles at 95°C for 1 minute and 58°C or 60°C for 1 minute. Real-time PCR data were expressed as fold change in fluorescence. Negative control experiments (samples without polymerase) were performed in parallel during different determinations to assess melting curve and assure equivalent assay conditions. cDNA products were also analyzed for purity by gel electrophoresis and sequencing. All assays were performed in triplicate and results reported as the mean ± SEM.

HFD experiment. After weaning, male mice were divided in two groups: one consuming a HFD; the other receiving a normal diet. The semipurified diet was purchased from Research Diets Inc. The HFD contains 45% fat by weight, whereas the control diet contains 5% fat (Research Diets Inc.). The energy densities of the low-fat diet and HFD were 4.07 kcal/g and 5.56 kcal/g, respectively. The fat source for the diets was coconut and soybean oil. Animals were single-housed in a temperature-controlled environment (25°C) with a 12-hour light/12-hour dark (18.00–06.00) photoperiod. Food intake and body weights were measured weekly. Body weight changes and food intake over the course of the experiment were analyzed by repeated-measures ANOVA followed by the Newman-Keuls post-hoc test.

Cloning and expression of PRCP. pMT/BiP/V5-His C was employed as the basal plasmid in vector construction. Human PRCP cDNA, lacking the first 391 base pairs of PRCP ($prcp_{nt391–1845}$), was subcloned into the vector at the *KpnI* and *EcoRI* multiple cloning site forming pMT/BiP/V5-His C-PRCP. The construction methods of the PRCP expression vector and the recombinant PRCP expression in Schneider 2 cells followed the standard protocols (17). The PRCP has a predicted molecular mass of 51 kDa ($rPRCP_{51}$).

Substrate inhibition assay. Samples containing 8 nM $rPRCP_{51}$ in 100 μl total volume were prepared in the absence or presence of increasing concentration of peptide α-$MSH_{1–13}$, α-$MSH_{1–12}$, or Ang II in HEPES carbonate buffer (137 mM NaCl, 3 mM KCl, 12 mM $NaHCO_3$, 14.7 mM HEPES, 5.5 mM dextrose, and 0.1% gelatin, pH 7.1, containing 10 mM $CaCl_2$, and 1 mM $MgCl_2$) in microtiter plate cuvette wells with previously absorbed HK at 1 μg/well and with 20 nM PK at 37°C. The ability of purified $rPRCP_{51}$ to activate PK bound to HK on plastic microtiter plates was determined in the absence or presence of increasing concentrations (0.001–1 mM) of the peptide (17, 18). After incubation, the wells were washed to remove unbound $rPRCP_{51}$ and peptide. Any formed kallikrein activity was determined by addition of 100 μl of S2302 (0.8 mM), and hydrolysis was observed at 405 nm for 1 hour at 37°C. The rate of hydrolysis was recorded at different concentrations of peptide and expressed as percent kallikrein activity remaining. Results were expressed as mean ± SEM of 3 or more experiments.

Intraperitoneal administration of α-MSH$_{1–13}$ and MTII to Prcp$^{gt/gt}$ and wild-type mice. Male wild-type and *Prcp$^{gt/gt}$* mice were used in this study. Animals were caged singly and injected with saline at the beginning of the dark phase for 3 days. For each mouse, food intake was measured at 4, 12, and 24 hours after injection. After 3 days, animals were divided in 6 groups: (a) wild-type mice receiving saline (n = 24); (b) wild-type mice receiving 200 nM α-MSH$_{1–13}$ in saline (n = 8); (c) wild-type mice receiving 200 nM MTII in saline (n = 8); (d) *Prcp$^{gt/gt}$* mice receiving saline (n = 24); (e) *Prcp$^{gt/gt}$* mice receiving 200 nM α-MSH$_{1–13}$ in saline (n = 8); (f) *Prcp$^{gt/gt}$* mice receiving 200 nM of MTII in saline (n = 8). For each experiment, means were compared between experimental groups using 1-way ANOVA followed by the Student-Newman-Keuls method. A level of confidence of $P < 0.05$ was used to determine significant differences.

MS analysis of the product of the PRCP reaction with α-MSH. The human rPRCP$_{51}$ was expressed and purified using the protocol described by Shariat-Madar et al. (13). Briefly, *PRCP* gene was obtained from cDNA using gene-specific primers. The elicited PCR product was sequenced and expressed a soluble protein of the expected size (51 kDa) and as an active enzyme in Schneider 2 (S2) insect cells. The 51-kDa recombinant PRCP denoted rPRCP$_{51}$.

Two micrograms of α-MSH$_{1–13}$ (Bachem H-1075, amide form; Bachem H-1070, free form) was incubated in the presence of 50 ng rPRCP$_{51}$ for 0 and 1 hour in a final volume of 100 μl acetate-phosphate buffer (0.01 mM sodium acetate and 50 mM sodium phosphate, pH 7.0) at 37°C. The incubation cocktail contained $CdCl_2$ (3 mM), 0.1 mM EDTA, 1,10-phenanthroline (10 mM), and 0.5 mM β-mercaptoethanol to exclude the participation of metalloproteases, aminopeptidase, and prolylendopeptidase. The reaction was stopped by 1 mM PMSF in a buffer (0.01 mM sodium acetate and 50 mM sodium phosphate, pH 5.8). Samples were then desalted using C18 ZipTip (Omix C18; Varian).

The reaction mixes were analyzed by mass spectrometry using a Surveyor HPLC system (Thermo Scientific), coupled to an LTQ FT Ultra Hybrid linear ion trap (7.0 T) Fourier transform ion cyclotron resonance (FT-ICR) mass spectrometer (Thermo Scientific). The HPLC was equipped with a microLC column (Magic C18 AQ, 3 μm, 200 Å, 150 × 1 mm; MICHROM Bioresources Inc.). Separation of peptides from the other molecules in the reaction mix was achieved by using a gradient from 5% to 45% mobile phase (0.1% formic acid in acetonitrile) in 0.1% formic acid, over 60 minutes. The electrospray voltage was 5 kV, and the accumulation of ions in the LTQ FT for MS was performed in the linear ion trap, with the automatic gain control target values set for wide selective ion monitoring.

Hypothalamic α-MSH and ACTH level measurements. Samples from both males and females were used in this study. Hypothalami (n = 14 for wild-type and n = 29 for *Prcp$^{gt/gt}$* mice) were dissected and immediately homogenized in 0.5 ml of 0.1N HCl and then centrifuged at 4,000 *g* and processed as previously described (26). Briefly, the supernatant was diluted with assay buffer and used for RIA. Protein content was determined by the Bradford method using BSA as the standard. α-MSH was measured with an antiserum (raised by our research group) that cross-reacts fully with desacetyl α-MSH but does not cross-react with ACTH or corticotropin-like intermediate-lobe peptide (CLIP) (27). The antiserum does not cross-react with the free acid form of α-MSH, which has not been amidated. ACTH was measured with an antiserum raised against synthetic ACTH$_{1–24}$, which is directed against the ACTH 5–18 sequence (IgG Corp.). The antiserum cross-reacts fully with POMC and Pro-ACTH. There is no cross-reactivity with α-MSH or CLIP. Statistical analysis was carried out with 2-tailed Student's t test.

In situ hybridization. The full-length *Prcp* mRNA was inserted in pCMV SPORT6 plasmid (Invitrogen). Linearized DNA was transcribed using T7 polymerase (antisense cRNA probe) and SP6 polymerase (sense cRNA probe) and labeled with DIG-labeled nucleotides according to the instructions provided in the kit (DIG RNA Labeling Kit; Roche). The labeled cRNA probe was then purified by passing the transcription reaction solution over a Sephadex G-50 column (GE Healthcare).

Brain sections from male and female mice were pretreated in PBS containing 4% paraformaldehyde for 7 minutes, rinsed in PBS, and washed 2 times (5 minutes each) in SSC 2× (150 mM NaCl, 15 mM sodium citrate, pH 7.2). Then, the sections were incubated with purified cRNA probe in hybridization buffer (50% formamide, 0.25 M sodium chloride, 1× Denhardt's solution, and 10% dextran sulfate) overnight at 50°C. After hybridization, the slides were washed briefly in washing buffer (0.1 M maleic acid, 0.15 M NaCl, 0.3% Tween 20, pH 7.2) and incubated in antibody (1:200; Roche) for 4 hours at room temperature. Detection of digoxigenin-labeled nucleic acids was carried out by enzyme-catalyzed color reaction according to the instructions provided in the kit (DIG Nucleic Acid Detection Kit; Roche). Sections were incubated as described above with hybridization solution containing the sense-strand probe synthesized by using SP6 polymerase to transcribe the coding strand of the DNA insert.

X-gal staining and immunocytochemistry. Male and female *Prcp$^{gt/gt}$* mice were perfused with 4% paraformaldehyde. Brains were sectioned with a vibratome (40 μm) and washed with PBS (137 mM NaCl, 2.7 mM KCl, 8 mM Na_2HPO_4, 2.6 mM KH_2PO_4) 4 times. Sections were then rinsed quickly once in cold PBS plus 2 mM $MgCl_2$ and incubated in the above solution for 10 minutes at 4°C. Permeabilization was performed by incubation in cold PBS with detergent (0.01% sodium desoxycholate and 0.02% NP40) for 10 minutes. Sections were then incubated overnight at 37°C in the staining solution containing 25 mM $K_3Fe(CN)_6$, 25 mM $K_4Fe(CN)_63H_2O$, 2 mM $MgCl_2$ in PBS and 1 mg/ml X-gal. Next, sections were rinsed in PBS and processed for immunocytochemistry. The following antisera were used: mouse β-endorphin (diluted 1:5,000; Chemicon), rabbit anti-MCH (diluted 1:12,000; Phoenix Pharmaceuticals Inc.), goat anti–Hcrt b (diluted 1:3,000; Santa Cruz Biotechnology Inc.), and mouse anti–tyrosine hydroxylase (TH; diluted 1:5,000; Sigma-Aldrich). Antisera were incubated overnight at room temperature. After several washes with phosphate buffer (PB), sections were incubated in their appropriate secondary antibody (biotinylated goat anti-rabbit, horse anti-mouse, horse anti-goat IgG; 1:250 in PB; Vector Laboratories) for 2 hours at room temperature, then rinsed in PB 3 times, 10 minutes each time, and incubated for 2 hours at room temperature with avidin-biotin-peroxidase (ABC, 1:50 in PB; ABC Elite Kit; Vector Laboratories Inc.). The immunolabeling was visualized with the nickel-diaminobenzidine (Ni-DAB) reaction (15 mg DAB, 165 μl 0.3% H_2O_2 in 30 ml PB) for 5–10 minutes at room temperature, resulting in a light brown reaction product.

Intracerebroventricular injection of α-MSH$_{1–13}$ and α-MSH$_{1–12}$. Eighteen male rats (200–250 g; Sprague-Dawley; Taconic) were used in this study. Animals with a third-ventricle cannulation were purchased from Taconic. Rats were caged singly and divided into 3 groups: animals injected with saline, animals injected with 2.5 μg α-MSH$_{1–13}$, and animals injected with 2.5 μg α-MSH$_{1–12}$. All the rats were fasted overnight. The next morning, the animals were injected, and a quantified amount of food was given and measured after 2 hours of refeeding (23).

Electrophysiology. Coronal hypothalamic brain slices from male and female (~300 μm) MC4R/GFP transgenic mice (gift of J.M. Friedman, Rockefeller University, New York, New York, USA; ref. 24) were prepared with a Vibratome. Slices were maintained at room temperature in artificial cerebrospinal fluid saturated with 95% O_2 and 5% CO_2. Slices were equilibrated in the recording chamber for 1 hour at 35°C in ACSF saturated with 95% O_2 and 5% CO_2 prior to recording. ACSF contained 124 mM NaCl; 3 mM KCl; 2 mM $CaCl_2$; 2 mM $MgCl_2$; 1.23 mM NaH_2PO_4; 26 mM $NaHCO_3$; 2.5 mM glucose, pH 7.4, with NaOH. An upright fluorescence/infrared microscope with long working distance objectives (BX51WI;

Olympus) and fluorescence filter sets for GFP (Chroma Technology Corp.) were used. Fluorescent MC4R-GFP neurons were selected, and a patch pipette (4–6 megohm resistance) was advanced onto the surface of the neuron by a micromanipulator (MP-225; Sutter). The pipette solution contained 128 mM K gluconate; 10 mM HEPES; 1 mM EGTA; 10 mM KCl; 1 mM $MgCl_2$; 0.3 mM $CaCl_2$; 2 mM (Mg)-ATP; 0.3 mM (Na)GTP, pH.7.4. Whole-cell patch clamp experiments were performed with a Multiclamp 700A amplifier (Axon Instruments, Molecular Devices). Whole-cell current clamp was used to monitor the effect of α-MSH_{1-13} (10 nM) or α-MSH_{1-12} (10 nM) on the membrane potential of recorded neurons held at resting membrane potential. All data were sampled at 3–10 kHz and filtered at 1–3 kHz with an Apple Macintosh computer using AxoGraph 4.9 (Axon Instruments, Molecular Devices). Electrophysiological data (n = 9 for each peptide) were analyzed with AxoGraph 4.9, plotted with IGOR Pro software (WaveMetrics), and presented as the mean ± SEM. Statistical analysis was performed by unpaired t test. The level of statistical significance was set at $P \leq 0.05$.

Intracerebroventricular injection of BPP. Twelve male rats (200–250 g; Sprague-Dawley; Taconic) were used in this study. Animals with a third-ventricle cannulation were purchased from Taconic. Rats were caged singly and divided into 2 groups: animals injected with 0.9 μg of BPP in 4 μl total volume and animals injected with the same volume of vehicle (2% methanol in artificial cerebrospinal fluid). A known amount of food was given to the animals and was weighed every 24 hours.

Intraperitoneal injection of BPP. For this study, 10 male *Lepob/ob* mice were used. Mice were injected at the beginning of the dark phase i.p. with a dose of 400 μg of BPP in 200 μl. Twenty-four hours later, food was measured and mice were injected with another dose of 400 μg of BPP; food intake was measured 24 hours later. Control mice were injected at the same times and with the same volume of vehicle (10% methanol in saline).

Dose-response curve of i.p. injection of ZPP. For this study, 10 male wild-type mice were used. Mice were fasted overnight and injected in the morning i.p. with either vehicle (10% methanol in saline) or 3 different doses of ZPP: 10, 40, and 100 mg/kg BW on a volume not greater than 200 μl. Food was provided and measured at 1, 2, 4, 8, and 24 hours. Significance of the drug effects at different time points was determined by 2-way ANOVA.

Intraperitoneal injection of ZPP. For this study, 10 male *Lepob/ob* mice were used. Mice were injected at the beginning of the dark phase i.p. with a dose of 100 mg/kg BW ZPP. The injection was repeated after 12 hours, and food intake was measured 12 hours after each injection. Control mice were injected at the same times and with the same volume of vehicle (10% methanol in saline).

SHU9119/ZPP administration. For this study, 24 male mice were fasted overnight and divided into the following groups: 8 mice injected i.c.v. with vehicle (1 μl) and i.p. with vehicle (10% methanol in saline; on a volume not greater than 200 μl volume); 8 mice injected i.c.v. with vehicle (1 μl) and i.p. with ZPP (100 mg/kg BW dissolved 10% methanol in saline; on a volume not greater than 200 μl); 8 mice injected i.c.v. with SHU9119 (6 nmol; 1 μl) and i.p. with ZPP (100 mg/kg BW dissolved 10% methanol in saline; on a volume not greater than 200 μl). Food intake was measured at 1, 2, and 4 hours. Significance of the drug effects at different time points was determined by 2-way ANOVA.

Statistics. Data are expressed as mean ± SEM unless otherwise indicated. Statistical differences among groups were determined by unpaired 2-tailed Student's t tests or repeated-measures ANOVA as specified throughout Methods. A level of confidence of $P < 0.05$ was employed for significance.

Acknowledgments

We thank Sue Bennet and Noreene Shibata for their mouse colony maintenance. We thank Andrea Kim for technical assistance in the measurements of hypothalamic α-MSH. We thank S. Wilk for the generous gift of BPP and J.M. Friedman for the use of GFP-MC4R mice. S. Diano is supported by NIH grant DK70039 and American Diabetes Association grant 1-08-RA-36; C.H. Warden is supported by NIH grant DK52581; A.H. Schmaier is supported by NIH grants HL52779, HL57346, and HL65194; S.L. Wardlaw is supported by NIH grant DK080003; and Z. Shariat-Madar is supported by NCRR/NIH grant P20RR021929.

Received for publication August 20, 2008, and accepted in revised form May 20, 2009.

Address correspondence to: Sabrina Diano, 333 Cedar Street LSOG 204B, New Haven, Connecticut 06510, USA. Phone: (203) 737-1216; Fax: (203) 785-4747; E-mail: sabrina.diano@yale.edu. Or to: Craig H. Warden, One Shields Avenue, 4303 Tupper Hall, Davis, California 95616-8635, USA. Phone: (530) 752-4187; Fax: (530) 752-3516; E-mail: chwarden@ucdavis.edu.

1. Muramatsu, Y., et al. 2005. Pnlip encoding pancreatic lipase is possible candidate for obesity QTL in the OLETF rat. *Biochem. Biophys. Res. Commun.* **331**:1270–1276.
2. Watanabe, T.K., et al. 2005. Mutated G-protein-coupled receptor GPR10 is responsible for the hyperphagia/dyslipidaemia/obesity locus of Dmo1 in the OLETF rat. *Clin. Exp. Pharmacol. Physiol.* **32**:355–366.
3. Stylianou, I.M., et al. 2005. Microarray gene expression analysis of the Fob3b obesity QTL identifies positional candidate gene Sqle and perturbed cholesterol and glycolysis pathways. *Physiol. Genomics.* **20**:224–232.
4. Williams, D.L., and Schwartz, M.W. 2005. The melanocortin system as a central integrator of direct and indirect controls of food intake. *Am. J. Physiol. Regul. Integr. Comp. Physiol.* **289**:R2–R3.
5. Wilkinson, C.W. 2006. Roles of acetylation and other post-translational modifications in melanocortin function and interactions with endorphins. *Peptides.* **27**:453–471.
6. Guo, L., Munzberg, H., Stuart, R.C., Nillni, E.A., and Bjorbaek, C. 2004. N-acetylation of hypothalamic alpha-melanocyte-stimulating hormone and regulation by leptin. *Proc. Natl. Acad. Sci. U. S. A.* **101**:11797–11802.
7. Diament, A.L., and Warden, C.H. 2004. Multiple linked mouse chromosome 7 loci influence body fat mass. *Int. J. Obes. Relat. Metab. Disord.* **28**:199–210.
8. McCarthy, J.J., et al. 2003. Evidence for substantial effect modification by gender in a large-scale genetic association study of the metabolic syndrome among coronary heart disease patients. *Hum. Genet.* **114**:87–98.
9. Jackson, R.S., et al. 1997. Obesity and impaired prohormone processing associated with mutations in the human prohormone convertase 1 gene. *Nat. Genet.* **16**:303–306.
10. Huszar, D., et al. 1997. Targeted disruption of the melanocortin-4 receptor results in obesity in mice. *Cell.* **88**:131–141.
11. Duhl, D.M., Vrieling, H., Miller, K.A., Wolff, G.L., and Barsh, G.S. 1994. Neomorphic agouti mutations in obese yellow mice. *Nat. Genet.* **8**:59–65.
12. Skarnes, W.C., Moss, J.E., Hurtley, S.M., and Beddington, R.S.P. 1995. Capturing genes encoding membrane and secreted proteins important for mouse development. *Proc. Natl. Acad. Sci. U. S. A.* **92**:6592–6596.
13. Shariat-Madar, Z., Mahdi, F., and Schmaier, A.H. 2002. Identification and characterization of prolylcarboxypeptidase as an endothelial cell prekallikrein activator. *J. Biol. Chem.* **277**:17962–17969.
14. Shariat-Madar, Z., Mahdi, F., and Schmaier, A.H. 2004. Recombinant prolylcarboxypeptidase activates plasma prekallikrein. *Blood.* **103**:4554–4561.
15. Odya, C.E., Marinkovic, D.V., Hammon, K.J., Stewart, T.A., and Erdos, E.G. 1978. Purification and properties of prolylcarboxypeptidase (angiotensinase C) from human kidney. *J. Biol. Chem.* **253**:5927–5931.
16. Fan, W., Boston, B.A., Kesterson, R.A., Hruby, V.J., and Cone, R.D. 1997. Role of melanocortinergic neurons in feeding and the agouti obesity syndrome. *Nature.* **385**:165–168.
17. Skofitsch, G., Jacobowitz, D.M., and Zamir, N. 1985. Immunohistochemical localization of a melanin concentrating hormone-like peptide in the rat brain. *Brain Res. Bull.* **15**:635–649.
18. Bittencourt, J.C., et al. 1992. The melanin-concentrating hormone system of the rat brain: an immuno- and hybridization histochemical characterization. *J. Comp. Neurol.* **319**:218–245.
19. de Lecea, L., et al. 1998. The hypocretins: hypothalamus-specific peptides with neuroexcitatory activity. *Proc. Natl. Acad. Sci. U. S. A.* **95**:322–327.
20. Sakurai, T., et al. 1998. Orexins and orexin receptors: a family of hypothalamic neuropeptides and

G protein–coupled receptors that regulate feeding behavior. *Cell.* **92**:1 page following 696.
21. Trivedi, P., Yu, H., MacNeil, D.J., Van der Ploeg, L.H., and Guan, X.M. 1998. Distribution of orexin receptor mRNA in the rat brain. *FEBS Lett.* **438**:71–75.
22. Horvath, T.L., Diano, S., and van den Pol, A.N. 1999. Synaptic interaction between hypocretin (orexin) and neuropeptide Y cells in the rodent and primate hypothalamus: a novel circuit implicated in metabolic and endocrine regulations. *J. Neurosci.* **19**:1072–1087.
23. Abbott, C.R., et al. 2000. Investigation of the melanocyte stimulating hormones on food intake. Lack of evidence to support a role for the melanocortin-3-receptor. *Brain Res.* **869**:203–210.
24. Liu, H., et al. 2003. Transgenic mice expressing green fluorescent protein under the control of the melanocortin-4 receptor promoter. *J. Neurosci.* **23**:7143–7154.
25. Wilk, S., and Orlowski, M. 1983. Inhibition of rabbit brain prolyl endopeptidase by n-benzyloxycarbonyl-prolyl-prolinal, a transition state aldehyde inhibitor. *J. Neurochem.* **41**:69–75.
26. Savontaus, E., et al. 2004. Metabolic effects of transgenic melanocyte-stimulating hormone overexpression in lean and obese mice. *Endocrinology.* **145**:3881–3891.
27. Wardlaw, S.L. 1986. Regulation of β-endorphin, corticotropin-like intermediate lobe peptide, and α-melanotropin-stimulating hormone in the hypothalamus by testosterone. *Endocrinology.* **119**:19–24.
28. Skidgel, R.A., and Erdos, E.G. 1998. Cellular carboxypeptidases. *Immunol. Rev.* **161**:129–141.
29. Jackman, H.L., et al. 1990. A peptidase in human platelets that deamidates tachykinins. Probable identity with the lysosomal "protective protein". *J. Biol. Chem.* **265**:11265–11272.
30. Broberger, C., Johansen, J., Johansson, C., Schalling, M., and Hokfelt, T. 1998. The neuropeptide Y/agouti gene-related protein (AGRP) brain circuitry in normal, anorectic, and monosodium glutamate-treated mice. *Proc. Natl. Acad. Sci. U. S. A.* **95**:15043–15048.
31. Singru, P.S., Sánchez, E., Fekete, C., and Lechan, R.M. 2007. Importance of melanocortin signaling in refeeding-induced neuronal activation and satiety. *Endocrinology.* **148**:638–646.